Applied Catalysis B: Environmental 146 (2014) 249–257

Contents lists available at ScienceDirect

Applied Catalysis B: Environmental

journal homepage: www.elsevier.com/locate/apcatb

# Kinetic and mechanistic study of the photocatalytic reforming of methanol over Pt/$TiO_2$ catalyst

Georgios N. Nomikos, Paraskevi Panagiotopoulou, Dimitris I. Kondarides*, Xenophon E. Verykios

*Department of Chemical Engineering, University of Patras, GR-26504 Patras, Greece*

ARTICLE INFO

*Article history:*
Received 1 November 2012
Received in revised form 9 February 2013
Accepted 5 March 2013
Available online 18 March 2013

*Keywords:*
Photo-reforming
Methanol
$TiO_2$
Platinum
Kinetics
Reaction mechanism

ABSTRACT

The kinetics and mechanism of photo-reforming reaction of methanol have been studied over Pt/$TiO_2$ suspensions irradiated with near-UV light ($\lambda_{max}$ = 365 nm). The effects of initial methanol concentration in solution ($C_{MeOH}$), photocatalyst content in suspension ($C_{cat}$) and incident light intensity ($I_0$) on the reaction rate have been investigated in detail. It has been found that the reaction rate depends strongly on methanol concentration and increases by more than two orders of magnitude with increase of $C_{MeOH}$ from zero to 1.0 M. The dependence of the reaction rate on $C_{MeOH}$ can be described by saturation-type kinetics according to the Langmuir–Hinselwood model. Increase of photocatalyst content in suspension results in an increase of the reaction rate, which tends to stabilize for $C_{cat} > 3\ g\ L^{-1}$. The rate of hydrogen evolution varies with incident light intensity in a manner which depends on the initial methanol concentration in solution. In particular, the order of the reaction with respect to $I_0$ is unity for $C_{MeOH}$ = 100 mM and 0.5 for $C_{MeOH}$ = 3.0 mM. Analysis of reaction intermediates in solution and on the photocatalyst surface indicates that, under the present experimental conditions, the reaction proceeds *via* progressive oxidation of adsorbed methoxy species to formaldehyde, dioxymethylene and formate. These species do not desorb from the photocatalyst surface but remain in the adsorbed mode until they are completely reformed to $H_2$ and $CO_2$.



## 1. Introduction

Semiconductor-mediated photo(electro)catalytic processes for the conversion and storage of solar energy have been the subject of numerous investigations in recent years, with emphasis given in the production of hydrogen *via* the water splitting reaction [1–5]. In spite of the intensive research efforts made in this field and of the large and excellent body of literature dealing with the development of highly active solar photocatalysts, there is currently no semiconductor material with the electronic properties and (photo)chemical stability required to catalyze efficiently the reaction under solar light irradiation [6,7]. In addition, the quantum efficiency and the rates of $H_2$ evolution are generally very small, mainly due to the occurrence of recombination reactions.

Some of the problems related to the lack of efficient solar light-responsive photocatalysts for water splitting can be overcome if the reaction takes place in the presence of organic sacrificial electron donors in solution. This method, which was first reported by Kawai and Sakata [8–12] and further investigated by several authors [13–24], combines reduction of water to $H_2$ with oxidation of organic compounds to $CO_2$ into a single process (photo-reforming) [13–15]. The kinetics of $H_2$ evolution is enhanced significantly because the organic substrate reacts rapidly and irreversibly with photogenerated holes thereby suppressing recombination reactions. Utilization of organic compounds as sacrificial electron donors may also permit the use of solar light-responsive, low bandgap semiconductor photocatalysts, which are otherwise not stable in aqueous environments [25,26]. Furthermore, photo-reforming reactions utilize not only the energy provided by incident photons, but also the chemical potential stored in the organic substrate itself, thereby resulting in increased overall efficiencies. Finally, if sacrificial compounds employed are pollutants or waste materials, the gain is double because the photo-reforming process leads to mineralization of environmentally harmful and/or non-recyclable substances with simultaneous production an energy-rich fuel.

Among the various organic compounds which may serve as sources of hydrogen, methanol has several advantages, including simple molecular structure, high hydrogen-to-carbon ratio and production from both fossil resources and biomass [27]. Although several methods have been developed for the conversion of methanol into hydrogen, such as decomposition, steam reforming, partial oxidation and oxidative steam reforming, these technologies can be applied at high temperatures and thus, require

* Corresponding author. Tel.: +30 2610 969527; fax: +30 2610 991527.
*E-mail address:* dimi@chemeng.upatras.gr (D.I. Kondarides).

0926-3373/$ – see front matter © 2013 Elsevier B.V. All rights reserved.
http://dx.doi.org/10.1016/j.apcatb.2013.03.018

significant amounts of heat, increasing the cost and complexity of the process. Thus, semiconductor-mediated photocatalytic reforming of methanol (1) has been studied in recent years as an environmentally friendly and low cost method for hydrogen production [21,27].

$$CH_3OH + H_2O \xrightarrow[Pt/TiO_2]{h\nu \geq E_{bg}} 3H_2 + CO_2 \quad (1)$$

It should be noted that the change in Gibbs free energy for reaction (1) is 9.3 kJ/mol and, therefore, the energy stored per absorbed photon in this 6-electron process is relatively small (0.016 eV). However, from a practical point of view, what is of interest in not the actual efficiency of the light-energy-storing process but the total energy that can be stored in the form of $H_2$ from investing a certain quantity of light energy. Methanol photo-reforming reaction may take place over UV-irradiated $TiO_2$ photocatalysts promoted by metal co-catalysts such as Pt [13,14,28–30], Au [21,27,31], Pd [32] and Cu [33]. Among these, $Pt/TiO_2$ exhibits the highest activity and selectivity for the reaction [13,14,29].

In the present work, the kinetics and mechanism of methanol photo-reforming reaction are investigated over irradiated $Pt/TiO_2$ photocatalyst suspensions. The effects of several operating parameters on the reaction rate are studied, including initial concentration of methanol in solution ($C_{MeOH}$), photocatalyst content in suspension ($C_{cat}$) and incident light intensity ($I_0$). Mechanistic aspects of the reaction are investigated by analyzing evolution of reaction intermediates and final products in the gas and liquid phases as well as on the photocatalyst surface employing GC, GC/MS and DRIFTS techniques.

## 2. Experimental

### 2.1. Catalyst preparation and characterization

The $Pt/TiO_2$ catalyst (0.5 wt.% Pt) employed was prepared by impregnation of titanium dioxide powder (Degussa P25) with an aqueous solution of $(NH_3)_2Pt(NO_2)_2$ (Alfa). The impregnated semiconductor was dried at 110 °C for 24 h, ground, sieved and finally reduced in $H_2$ flow at 300 °C for 2 h. The photocatalyst was characterized with respect to its specific surface area (41 $m^2\,g^{-1}$), metal dispersion (40.7%) and anatase-to-rutile content (75–25%), employing nitrogen physisorption at the temperature of liquid nitrogen, selective chemisorption of $H_2$ at 25 °C and X-ray diffraction (XRD), respectively. Details on the equipment and procedures used for catalyst preparation and characterization can be found elsewhere [24,34].

### 2.2. Apparatus and procedures

Photocatalytic experiments were carried out using an experimental setup, which consists of a light source, the photoreactor and the analysis system. The light source is of LED type (Nichia, model NCSU033A (T)) that emits near-UV light in a narrow range of wavelengths ($\lambda_{max}$ = 365 nm) close to the absorption threshold of $TiO_2$ ($\lambda_{th}$ = 390 nm). The quartz photoreactor is of cubic shape with flat optical windows (40 mm × 40 mm) and a top cover with connections for inlet/outlet of an inert gas (Ar) that flows through the suspension and serves as a means of collecting gaseous reaction products and carrying them into the on-line analysis system. The headspace of the reactor, including the volume of tubing up to the analysis system, is *ca.* 250 $cm^3$. The latter comprises a gas chromatograph (Varian CP3800) and an infrared analyzer (BINOS) that enable continuous monitoring of $H_2$ and $CO_2$, respectively, evolving at the reactor effluent. The incident light intensity was measured with the use of a power meter equipped with a photodiode detector (Oriel).

In a typical experiment, 60 mL of an aqueous methanol solution of known concentration is placed in the reactor, followed by addition of an amount of photocatalyst (usually 80 mg) under continuous stirring. The reactor is then sealed and Ar flow (20 $cm^3\,min^{-1}$) is permitted for about 2 h to ensure complete removal of atmospheric oxygen from the solution, reactor and tubing. Subsequently, the suspension is exposed to light (at $t = 0$) under continuous stirring and reaction products in the gas phase are recorded at the desired time intervals.

### 2.3. Analytical methods

Identification and quantification of reactant and intermediates in the liquid phase has been achieved in separate experiments where the reaction was stopped at the desired irradiation times, the suspension was collected, filtered and stored in sealed vials in a refrigerator. The solid residue collected at the filter was dried under vacuum at 70 °C and stored for further analysis. Analysis of compounds in solution has been achieved with the use of a gas chromatography–mass spectrometry (GC/MS) system. The GC (Hewlett-Packard 6890) is equipped with an HP-INNOWax capillary column (30 m × 0.25 mm id × 0.25 μm film thickness) and interfaced directly to the MS (HP 5973) used as a detector. Identification of the GC/MS spectral features has been achieved with the use of a built-in library. Response factors were determined with the use of self-prepared solutions of known concentration.

The *ex situ* DRIFT spectra of photocatalyst powders collected at various irradiation times were recorded using a Nicolet 6700 apparatus equipped with a diffuse reflectance (DRIFT) cell (Spectra Tech), an MCT detector and a KBr beam splitter [35]. Spectra were obtained with a 32-scan data acquisition at a resolution of 4 $cm^{-1}$ over samples exposed to the atmosphere at room temperature. The spectrum obtained for $Pt/TiO_2$ catalyst subjected to a similar pretreatment (suspended in water, filtered, dried, *etc.*) but not exposed to UV-light was used as a background reference.

The amount of carbon-containing species formed on the photocatalyst surface under photo-reforming reaction conditions was estimated with the use of temperature-programmed oxidation (TPO) method, using the apparatus and following the procedures that have been described in detail elsewhere [35,36]. In a typical experiment, an amount of photocatalyst sample (~20 mg), collected and pre-treated as described above, was placed in a quartz microreactor and exposed to a 3% $O_2$/He flow (30 $cm^3\,min^{-1}$) for 10 min. The catalyst was then heated linearly ($\beta$ = 30 °C $min^{-1}$) up to 750 °C under the same flow and the effluent gas composition was monitored on-line with the use of an Omnistar/Pfeiffer Vacuum mass spectrometer (MS). The response of the mass spectrometer was calibrated against standard mixtures of accurately known composition.

## 3. Results and discussion

### 3.1. Effects of operating conditions on reaction rate

#### 3.1.1. Methanol concentration in solution

Typical results obtained over irradiated photocatalyst suspensions in the absence and in the presence of small concentrations of methanol in solution (0.0–10 mM) are presented in Fig. 1, where the rates of evolution of $H_2$ (Fig. 1A) and $CO_2$ (Fig. 1B) are plotted as functions of irradiation time. It is observed that in absence of methanol, *i.e.*, when pure water is employed, the hydrogen production rate ($r_{H_2}$) goes through a weak maximum of *ca.* 0.05 mol $min^{-1}$ at $t$ = 50 min and then decreases to a much lower pseudo-steady

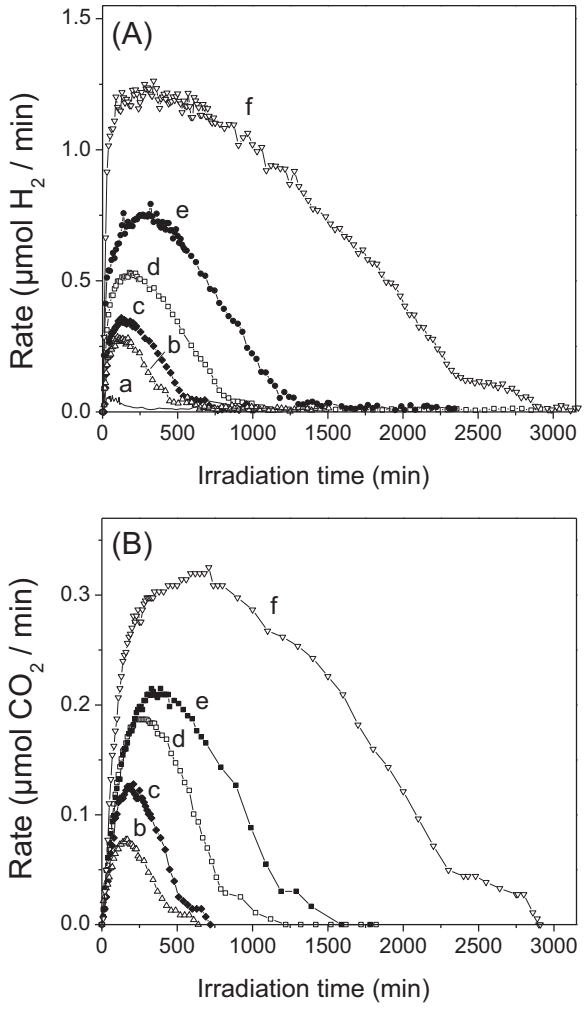


**Fig. 1.** Rates of (A) $H_2$ and (B) $CO_2$ evolution as functions of irradiation time obtained over photocatalyst suspensions of variable methanol concentration: (a) 0.0 mM; (b) 0.37 mM; (c) 0.75 mM; (d) 1.5 mM; (e) 3.0 mM; (f) 10 mM. Other experimental conditions: $C_{cat} = 1.33\ g\ L^{-1}$; $I_0 = 3\ mW\ cm^{-2}$.

state value (trace a). It should be noted that under these conditions evolution of $H_2$ is not accompanied by production of $CO_2$ and therefore the presence of organic contaminants may be excluded. This indicates that Pt/$TiO_2$ shows some activity for the water splitting reaction, in agreement with results of our previous studies [13–16].

Addition of a small amount of methanol in solution (0.37 mM) results in a significant increase of $r_{H_2}$ (trace b) the maximum of which (0.29 mol $min^{-1}$) is approximately 6 times higher, compared to that obtained from pure water. Prolonged exposure to light results in a progressive decrease of $r_{H_2}$ to the levels obtained in the absence of methanol in solution. It should be kept in mind that the monotonic increase of $r_{H_2}$ observed immediately after exposure to light, as well as the presence of a maximum in the rate curve ($r_{max}$), are experimental artifacts. This can be understood by considering that the dead space downstream the reactor (250 $cm^3$) is relatively high compared to the flow rate of Ar (20 $cm^3\ min^{-1}$), which carries gas phase products to the analysis system. It has been estimated that a time period of *ca.* 1 h is required for the reactor effluent to purge this volume, which is in agreement with the time of appearance of the rate maximum in the $H_2$-rate curves (Fig. 1A). Thus, $r_{max}$ represents, practically, the initial rate of $H_2$ production.

Production of hydrogen is accompanied by evolution of $CO_2$ in the gas phase, the rate of which ($r_{CO_2}$) goes through a maximum and then drops to zero after about 600 min under irradiation (Fig. 1B, trace b). Increase of the initial methanol concentration in solution in the range of 0.37–10 mM results in a monotonic increase of the rate maxima of both products (traces b–f). This is accompanied by an increase of the total quantities of $H_2$ and $CO_2$ produced, which can be determined by integrating the corresponding rate curves. As shown in Fig. 2, the total amounts of $H_2$ and $CO_2$ produced are in excellent agreement with those predicted by the stoichiometry of reaction (1), thereby confirming that the overall reaction can be described as photo-reforming of methanol.

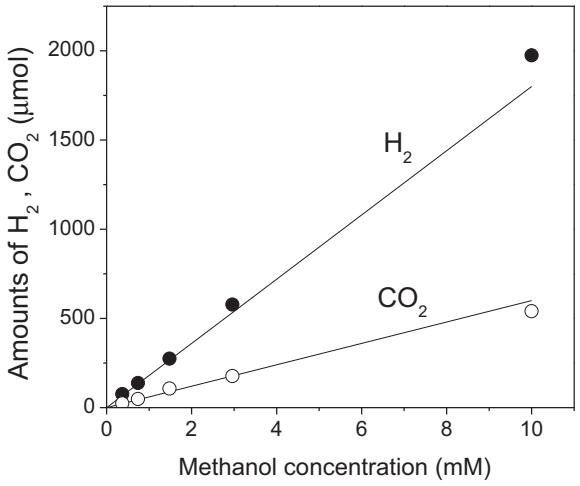


**Fig. 2.** Total amounts of $H_2$ and $CO_2$ produced (symbols) compared to the values predicted by the stoichiometry of the methanol photo-reforming reaction (1) (lines). Data obtained from Fig. 1.

Results of Fig. 1 can be explained by considering that methanol serves as a sacrificial electron donor, which removes rapidly and irreversibly photogenerated holes ($h^+$) and other oxidizing agents (*e.g.*, $^{\bullet}OH$, $O_2^{\bullet -}$, $HO_2^{\bullet}$, $H_2O_2$) which may be formed under conditions of photocatalytic cleavage of water [23]. Thus, the rates of back-reactions, especially electron–hole recombination, which are mainly responsible for the low efficiency of the process, are suppressed and the rate of $H_2$ production is enhanced significantly [13–18,23]. When the sacrificial compound in solution is fully consumed, the photogenerated oxidants cannot be removed efficiently from the photocatalyst surface and, as a result, the rate of hydrogen production drops to the low levels obtained from pure water.

The rate curves presented in Fig. 1 were obtained with the use of relatively low initial concentrations of methanol (0.0–10 mM) in order to achieve complete reformation of the reactant in a reasonable period of time. Qualitatively similar results were obtained in the presence of higher concentrations of methanol, namely 100 mM (Fig. 8, *vide infra*), 500 mM and 1000 mM (not shown for brevity). Results obtained (including those shown in Fig. 1) are summarized in Fig. 3, where the maximum rate of $H_2$ evolution ($r_{max}$) is plotted as a function of initial methanol concentration in solution ($C_{MeOH}$). It is observed that $r_{max}$ depends strongly on $C_{MeOH}$ and increases by more than two orders of magnitude (*i.e.*, from 0.05 to 5.34 mol $H_2\ min^{-1}$) with increase of $C_{MeOH}$ from zero to 1.0 M. The dependence of $r_{max}$ on $C_{MeOH}$ is very strong for low methanol concentrations and becomes progressively weaker with increase of $C_{MeOH}$. Qualitatively similar results have been reported previously for the photo-reforming of methanol and glucose [32,37–39]. In general, this behavior can be described by saturation-type kinetics according to the Langmuir–Hinselwood (LH) model, which is very often used to approximate the dependence of photocatalytic reaction rates on substrate concentration [40–42]

$$r = \frac{kKC}{1 + KC} \quad (2)$$

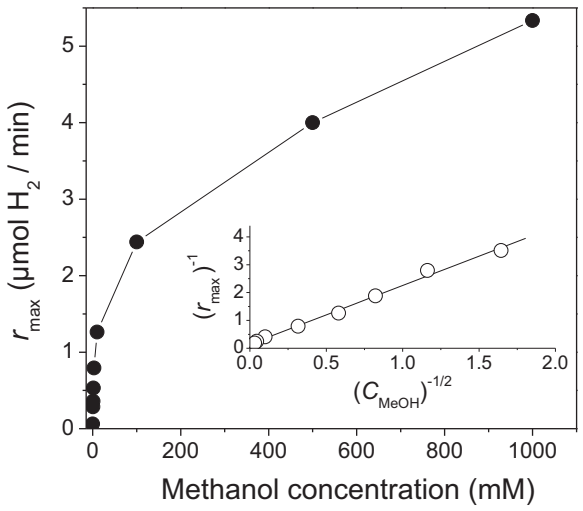


**Fig. 3.** Maximum rate of hydrogen evolution ($r_{max}$) as a function of initial methanol concentration in solution ($C_{MeOH}$). *Inset*: plot of the same data points according to the linearized Langmuir–Hinselwood model (see text for details).

where $k$ is an apparent rate constant and $K$ is the equilibrium constant.

The operability of the LH kinetic model can be tested by plotting the inverse reaction rate, $1/r$, as a function of the inverse reactant concentration, $1/C$ (or $1/C^{1/2}$ for dissociative adsorption), which should give a straight line. In the present case, a linear dependence of $1/r_{max}$ on $(1/C_{MeOH})^{1/2}$ is observed (inset of Fig. 3). This indicates that the (apparent) reaction rate can be described according to a LH model in which the active form of the reactant (methanol) is in a dissociative state.

### 3.1.2. Photocatalyst content in suspension

The effect of photocatalyst concentration ($C_{cat}$) on the reaction rate has been investigated for two different initial concentrations of methanol (3.0 mM and 100 mM) under a constant incident light intensity of 3 mW cm$^{-2}$. Results obtained for $C_{MeOH}$ = 3.0 mM are summarized Fig. 4A, which shows the rate curves of $H_2$ evolution for $C_{cat}$ varying between 0.17 and 5.0 g L$^{-1}$. It is observed that, in all cases, $r_{H_2}$ goes through a maximum and then drops to very low values when reactant and intermediates are completely oxidized to $CO_2$. The rate maximum increases with increase of $C_{cat}$ up to *ca.* 2.64 g L$^{-1}$ (trace e), which is accompanied by a decrease of the irradiation time required for the complete reformation of methanol in the solution. Further increase of $C_{cat}$ up to 5.0 g L$^{-1}$ does not improve significantly the reaction rate (traces f and g). Qualitatively similar results were obtained for $CO_2$ evolution (not shown for brevity). The total amount of $H_2$ (and $CO_2$) produced was practically the same in all cases, because the same initial concentration of methanol was used in this set of experiments (3.0 mM). Results of similar experiments conducted with the use of a higher concentration of methanol (100 mM) are shown in Fig. 4B. It is observed that the dependence of $r_{H_2}$ curves on $C_{cat}$ is qualitatively similar to that obtained for $C_{MeOH}$ = 3.0 mM (Fig. 4A).

The dependence of $r_{max}$ on $C_{cat}$ for the two sets of experiments presented in Fig. 4 is shown in Fig. 5. It is observed that for low photocatalyst loadings $r_{max}$ increases with increase of $C_{cat}$ and then tends to level off. This can be understood by considering that the reaction rate is determined by both the number of surface active sites and the light transmission in suspension [43,44]. For low photocatalyst concentrations, the reaction is controlled by the number of surface active sites that absorb incident photons and, therefore, the rate increases with increase of photocatalyst loading. This region corresponds to the true heterogeneous catalytic

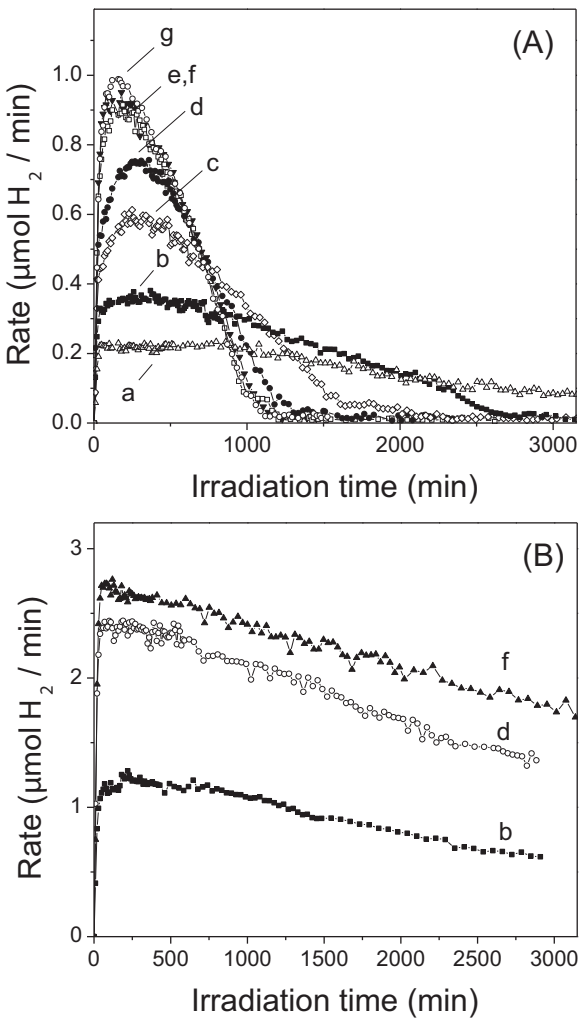


**Fig. 4.** Effect of photocatalyst content ($C_{cat}$) on the rate of $H_2$ evolution for two different initial concentrations of methanol in solution: (A) 3.0 mM; (B) 100 mM. $C_{cat}$ (g L$^{-1}$): (a) 0.17; (b) 0.33; (c) 0.67; (d) 1.33; (e) 2.64; (f) 4.0; (g) 5.0. $I_0$ = 3 mW cm$^{-2}$.

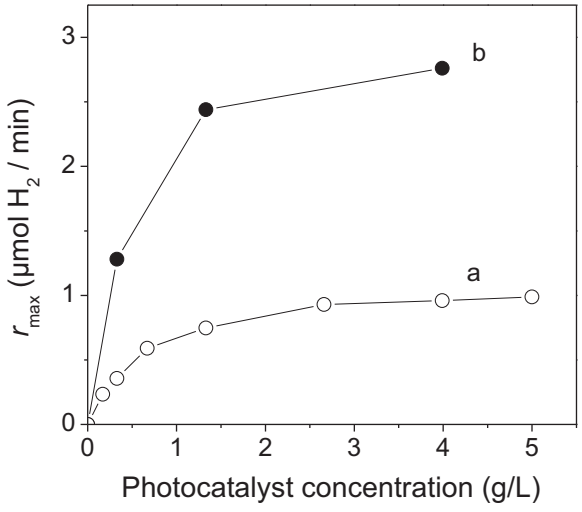


**Fig. 5.** Effect of photocatalyst content on the maximum rate of $H_2$ evolution for initial methanol concentrations of (a) 3.0 mM and (b) 100 mM (data obtained from Fig. 4).

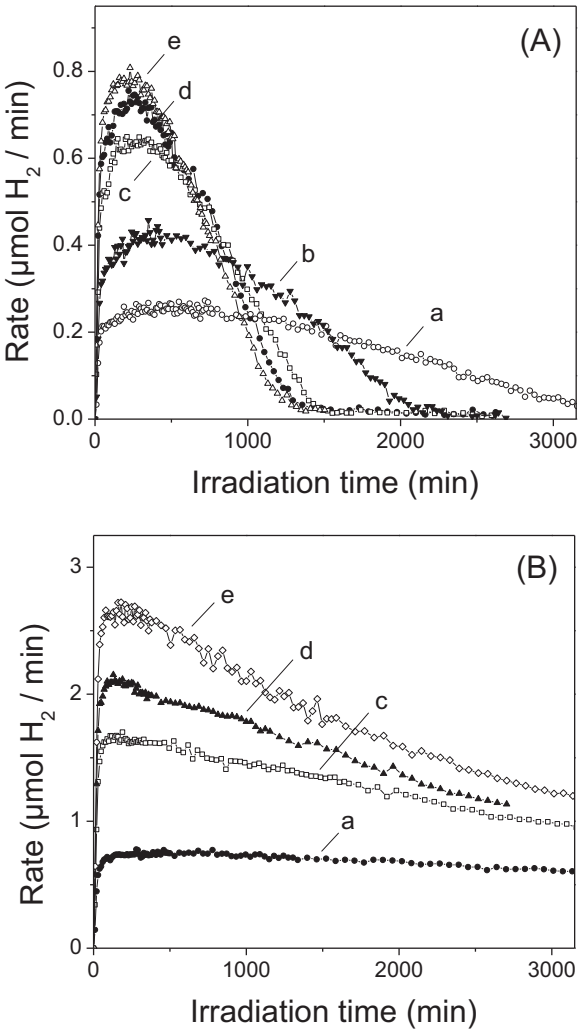


**Fig. 6.** Effect of incident light intensity ($I_0$) on the rate of hydrogen evolution for photocatalyst suspensions of initial methanol concentrations of (A) 3.0 mM and (B) 100 mM. $I_0$ (mW cm$^{-2}$): (a) 0.5; (b) 1.0); (c) 1.9; (d) 2.3; (e) 3.0. $C_{cat}$ = 1.33 g L$^{-1}$.

regime and its limit represents the maximum amount of photocatalyst in which the surface of all particles is totally illuminated [40]. Above this limit (*ca.* 2.0 g L$^{-1}$ in the present case), where the opacity of the suspension increases and a substantial amount of light is scattered by photocatalyst particles, the reaction rate either levels off (Fig. 5) or even decreases [40]. In essence, the photocatalyst particles themselves act as an inner filter despite good stirring of the dispersion during irradiation [45,46]. The optimal photocatalyst concentration, for which the whole photocatalyst surface is effectively irradiated, depends on reaction conditions and the geometrical characteristics of the light source-photoreactor system [40,43–45].

### 3.1.3. Incident light intensity

The effects of incident light intensity on the reaction rate have been investigated in the range of $I_0$ = 0.5–3.0 mW cm$^{-2}$ keeping constant the concentration of the photocatalyst in suspension (1.33 g L$^{-1}$). Results obtained with the use of a small initial methanol concentration (3.0 mM) are shown in Fig. 6A, where $r_{H_2}$ is plotted as a function of irradiation time. It is observed that increase of $I_0$ from 0.5 to 2.3 mW cm$^{-2}$ results in an increase of the maximum rate of hydrogen production and in a decrease of the time required for complete reformation of methanol and reaction intermediates (traces a–d). Further increase of $I_0$ to 3.0 mW cm$^{-2}$ does

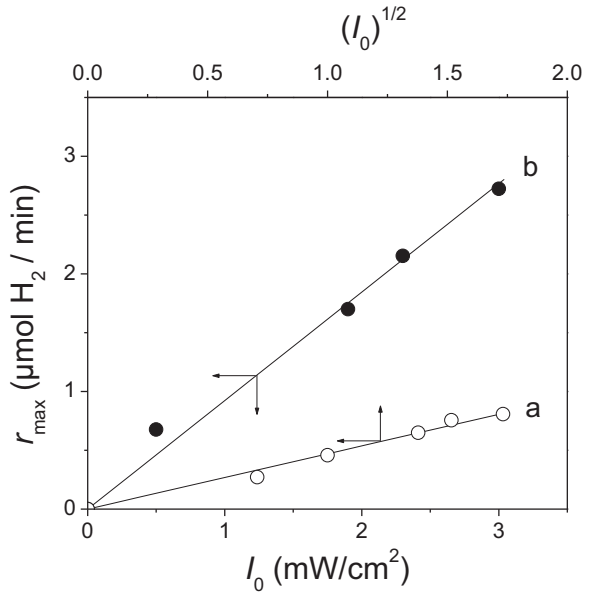


**Fig. 7.** Effect of the incident light intensity ($I_0$) on the maximum rate of hydrogen evolution for initial methanol concentrations of (a) 3.0 mM and (b) 100 mM (data obtained from Fig. 6).

not improve significantly the reaction rate (trace e). Interestingly, for higher initial methanol concentration in solution (100 mM), the hydrogen production rate increases monotonically with increase of $I_0$ (Fig. 6B).

Results obtained with the use of variable incident light intensities are summarized in Fig. 7, which shows the dependence of $r_{max}$ on $I_0$ for the two different initial methanol concentrations investigated. It is observed that for $C_{MeOH}$ = 100 mM the rate scales linearly with $I_0$ (curve b) whereas for $C_{MeOH}$ = 3.0 mM $r_{max}$ is proportional to the square-root of $I_0$ (curve a). This behavior is in general agreement with results of previous studies, which show that the dependence of the rate of heterogeneous photocatalytic reactions on incident light intensity can be usually approximated by either linear [47,48] or square-root [47–49] functions. The type of approximation is known to depend on the magnitude of $I_0$. Under weak illumination, band bending in the space-charge layer of the semiconductor is sufficiently high to result in efficient separation of the photogenerated electron–hole pairs. Thus, the rate of electron–hole recombination is relatively small, photogenerated charge carriers are mainly

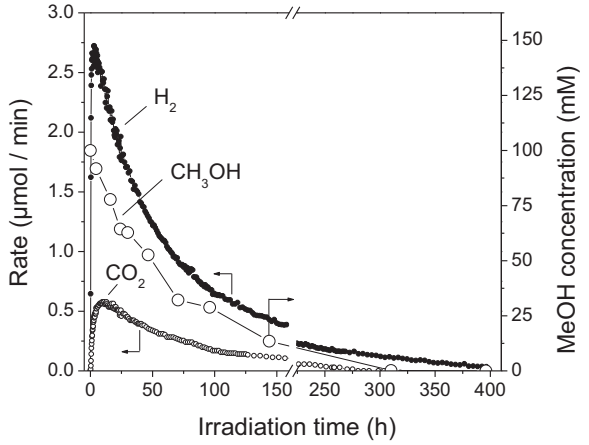


**Fig. 8.** Rates of $H_2$ and $CO_2$ evolution in the gas phase and methanol concentration in solution as functions of irradiation time. $C_{MeOH}$ = 100 mM. $C_{cat}$ = 1.33 g L$^{-1}$, $I_0$ = 3 mW cm$^{-2}$.

consumed by chemical reactions, and the rate is first order with respect to $I_0$. However, above a certain value of $I_0$, the reaction rate becomes proportional to the square root of light intensity. This is because with increasing light intensity, the extent of band bending tends to decrease and the surface reactions strongly compete with processes involving electron–hole recombination. Under these conditions, the rate becomes half order with respect to $I_0$. For very high light intensities the order of reaction rate on $I_0$ is nearly zero, because surface intrinsic kinetics are so rapid that the observed reaction rate is limited by the diffusional supply of reactants from the liquid phase [49]. Regarding the observed interdependence of the reaction rate on concentration and light intensity (Fig. 7), it commonly occurs in photocatalytic processes [41,42]. In particular, the linear dependence of the reaction rate on light intensity is seen when the dependence of the reaction rate on concentration is near saturation (*i.e.*, when $KC \gg 1$ in Eq. (2)).

### 3.2. Mechanistic study

#### 3.2.1. Reaction products in the gas phase

The mechanism of the photo-reforming reaction was investigated with the use of a methanol solution of relatively high concentration (100 mM) in order to allow detection of intermediate species in the liquid phase. Results obtained from the analysis of the gas phase at the reactor effluent are summarized in Fig. 8, where the rates of $H_2$ ($r_{H_2}$) and $CO_2$ ($r_{CO_2}$) evolution are plotted as functions of irradiation time. No other reaction products have been detected in the gas phase under the present conditions. It is observed that the rate of hydrogen production goes through a maximum of 2.7 μmol $min^{-1}$ at *ca.* 150 min under irradiation. Prolonged exposure to illumination results in a progressive decrease of $r_{H_2}$, which eventually drops to pseudo-steady state values comparable to those obtained from pure water. Production of $H_2$ is accompanied by evolution of $CO_2$, the rate of which goes through a relatively broad maximum (0.57 μmol $min^{-1}$) at *ca.* 7–14 h under illumination and then gradually decreases with time. Under these experimental conditions, the irradiation time required for completion of the photo-reforming reaction is about 400 h. It should be noted that the total amounts of $H_2$ and $CO_2$ produced throughout the experiment were 11.7 and 3.4 mmol, respectively, which are substantially lower, compared to those predicted by the stoichiometry of reaction (1) (18 mmol $H_2$, 6 mmol $CO_2$). This is because part of methanol in solution was gradually transferred to the gas phase over the long duration of the experiment, due to the relatively high vapour pressure of the molecule. The presence of trace amounts of methanol in the reactor effluent was confirmed in separate experiments where the gaseous products were analyzed with the use of a gas chromatograph (Shimadzu GC 14A) operating with He as carrier gas. In addition, an amount of carbon-containing species was found to remain adsorbed on the photocatalyst surface after completion of the experiment (see below).

#### 3.2.2. Reaction intermediates in the liquid phase and on the photocatalyst surface

Conversion of methanol and evolution of reaction intermediates in solution and on the photocatalyst surface have been investigated with the use of GC, GC/MS and DRIFTS techniques. As shown in Fig. 8, the concentration of methanol in solution decreases progressively with time and diminishes after *ca.* 400 h. Interestingly, no reaction intermediates, such as formic acid and formaldehyde that have been reported in previous investigations [22,30] were detected in the liquid phase. It should be noted, however, that the latter studies were obtained either in the gas phase [22] or with the use of a different type of $TiO_2$ [30]. This indicates that, under the present conditions, reaction intermediates do not evolve in the liquid phase but remain adsorbed on the photocatalyst surface until they are completely oxidized toward $CO_2$.

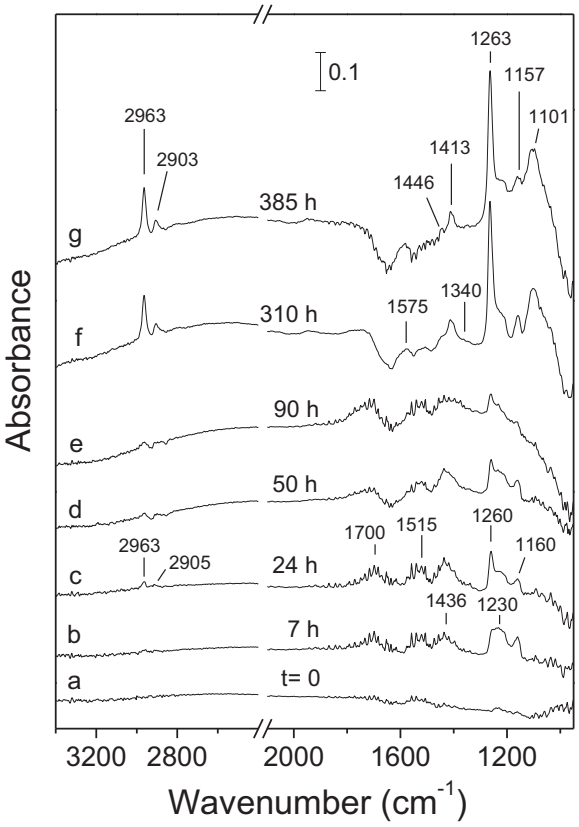


**Fig. 9.** DRIFT spectra obtained over $Pt/TiO_2$ photocatalyst powders collected at the indicated irradiation times under conditions of methanol photoreforming reaction.

In order to confirm the above argument, the progress of the reaction on the photocatalyst surface was monitored with the use of DRIFTS. The *ex situ* spectra obtained over samples collected at different irradiation times are shown in Fig. 9. It should be reminded that prior to recording the spectra, the photocatalyst samples were dried under vacuum at 70 °C. This pretreatment, which resulted in desorption of water and weakly adsorbed species, may explain the reason why the spectrum obtained at $t = 0$ (trace a) does not contain any bands characteristic of adsorbed methanol. Exposure of the $Pt/TiO_2$ catalyst to light under photo-reforming reaction conditions results in the development of several bands in the C–H stretching frequency region (3100–2700 $cm^{-1}$) and in the C–H deformation and C–O stretching regions (1700–1000 $cm^{-1}$), the intensity of which increases progressively with irradiation time (traces b–g). The peaks located at 2963 and 2905 $cm^{-1}$, which are discernible after 7 h under irradiation (trace b) and are clearly resolved after more than 90 h (traces f and g), can be assigned to C–H stretching vibrations of adsorbed species containing methyl ($CH_3$) and methylene ($CH_2$) groups [50–52].

Spectra presented in Fig. 9 may contain contributions from species adsorbed on both the $TiO_2$ surface and the Pt crystallites. However, due to the relatively low Pt content, it may be argued that the observed bands are mainly due to species adsorbed on $TiO_2$. The large number of overlapping peaks detected below 1750 $cm^{-1}$ makes difficult the determination of their accurate positions and relative intensities and, therefore, a detailed assignment of the corresponding surface species is not possible. However, based on literature results, most of these peaks can be attributed to adsorbed formaldehyde and formate species [53–58]. In order to confirm this, two additional experiments were carried out, in which 60 mL of an

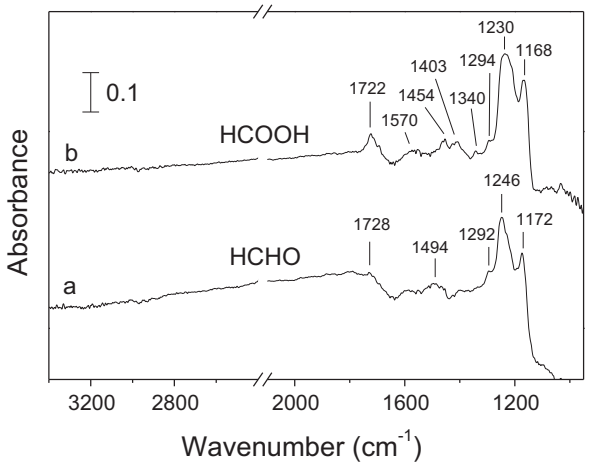


**Fig. 10.** DRIFT spectra obtained over the $Pt/TiO_2$ photocatalyst following interaction with aqueous solutions of formic acid or formaldehyde.

aqueous formic acid or formaldehyde solution ($C$ = 100 mM) were placed in the reactor, followed by addition of 80 mg of $Pt/TiO_2$ catalyst. The suspensions were left in the dark for 24 h under continuous stirring followed by filtration and drying of the photocatalyst under vacuum at 70 °C. As shown in Fig. 10, the DRIFT spectra obtained from these samples are qualitatively similar to those obtained over the photocatalyst samples collected after prolonged exposure to irradiation (Fig. 9). In particular, the bands located at *ca.* 1700, 1515, 1260 and 1160 $cm^{-1}$, which dominate at low irradiation times (Fig. 9, traces b–e) can be attributed to $\nu$(CO) stretching, $\omega(CH_2)$ wagging, $\gamma(CH_2)$ rocking and $\tau(CH_2)$ modes of adsorbed formaldehyde ($CH_2O_{(a)}$), respectively [53–55]. For irradiation times longer than 90 h two new bands located at *ca.* 1575 and 1340 $cm^{-1}$ become discernible, which can be assigned to adsorbed formate species [29,36,53–58]. Regarding the bands at 1446, 1413 and 1101 $cm^{-1}$, which clearly evolve after more than 90 h (traces f and g), they have been previously attributed to $\delta(CH_2)$, $\omega(CH_2)$ and $\rho(CH_2)$ of dioxymethylene ($H_2CO_{2(a)}$) species [29,53,54,56].

Results of Fig. 9 demonstrate that increase of irradiation time results in an increase of the population of species adsorbed on the photocatalyst surface, which is more evident for irradiation periods longer than 90 h (traces f and g). In order to verify this, the amount of carbon-containing species deposited on the photocatalyst surface was estimated by temperature-programmed oxidation (TPO) method. Representative results obtained over the $Pt/TiO_2$ catalyst sample collected after 385 h under irradiation are shown in the TPO pattern of Fig. 11A, where the response of $CO_2$ is plotted as a function of temperature. It is observed that the profile of $CO_2$ exhibits three peaks with their maxima located at *ca.* 225, 370 and 525 °C, indicating that there are at least three distinct carbon-containing species on the photocatalyst surface.

Qualitatively similar TPO profiles were obtained over photocatalyst samples collected after exposure to photo-reforming reaction conditions for variable irradiation times. Results obtained (not shown for brevity) are summarized in Fig. 11B, where the total amount of C-containing species, desorbed as $CO_2$ in TPO experiments, is plotted as a function of irradiation time. It is observed that the amount of $CO_2$ produced acquires a relatively small value of *ca.* 0.035 mmol/$g_{cat}$ for $t$ = 7–90 h. Further exposure to light results in a significant increase of the amount of $CO_2$ produced, which reaches a value of 0.13 mmol/$g_{cat}$ for $t$ = 400 h (Fig. 11B). This observation is in agreement with results presented in Fig. 9, which show a significant increase in the intensities of bands attributed to adsorbed species for irradiation times longer than *ca.* 90 h (traces f and g).

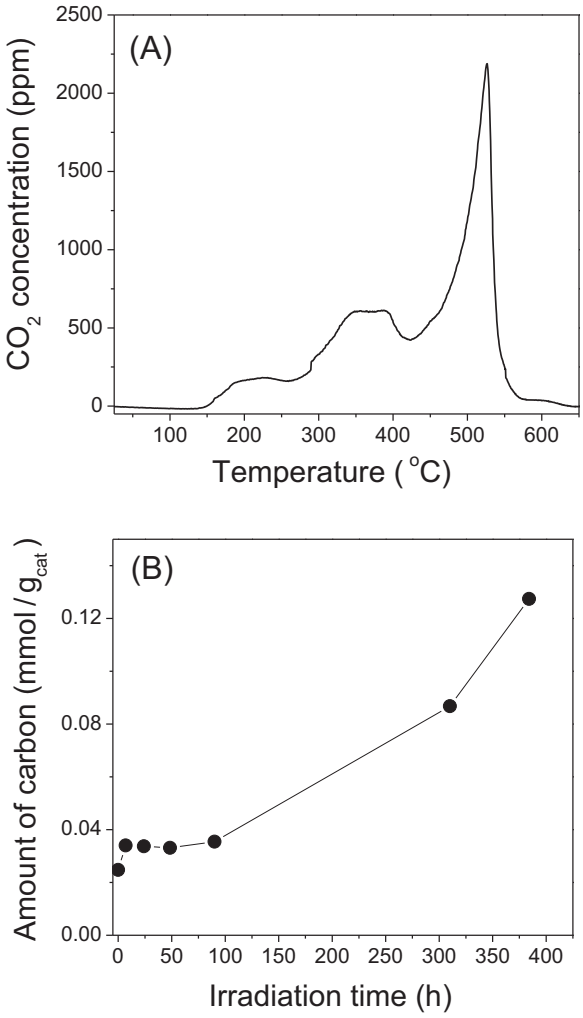


**Fig. 11.** (A) Response of $CO_2$ produced during temperature programmed oxidation with 3%$O_2$ (in He) over a $Pt/TiO_2$ photocatalyst exposed to irradiation for 385 h under conditions of methanol photo-reforming. (B) Total amount of carbon deposited on the photocatalyst surface under conditions of methanol photo-reforming as a function of irradiation time, estimated from TPO experiments.

### 3.3. Mechanistic implications

Results of mechanistic studies presented in Figs. 8–11 can be understood by considering that, as in all photocatalytic reactions, methanol photo-reforming is initiated by excitation of the semiconductor by photons of ultra bandgap energy, which results in the promotion of an electron from the valence band to the conduction band of the semiconductor [59]. Photogenerated electrons are trapped by the dispersed Pt crystallites [6] whereas photogenerated holes remain on $TiO_2$:

$$Pt\text{-}TiO_2 \xrightarrow{h\nu \geq E_{bg}} Pt(e^-) - TiO_2(h^+) \quad (3)$$

Charge separation results in efficient suppression of electron–hole recombination reactions that limit efficiency, and in increased lifetimes of photogenerated carriers which have the opportunity to react with adsorbed species and initiate redox reactions [59].

In our previous studies it was shown that deposition of Pt crystallites on the $TiO_2$ surface is a prerequisite for the efficient production of $H_2$ by photo-reforming of organic substrates [13–16,24]. It was concluded that, in addition to trapping of photogenerated electrons, Pt deposits enhance the rate of hydrogen evolution by

decreasing the overpotential for the reduction of protons to hydrogen [24]:

$$e^- + H^+ \rightarrow \tfrac{1}{2}H_2 \quad (4)$$

Dispersed Pt crystallites may also act as thermal catalysts by providing sites for adsorbed species and reaction intermediates and by promoting dehydrogenation reactions discussed below [24]. Regarding photogenerated holes, they can oxidize adsorbed organic species, either directly or indirectly, *via* intermediate formation of hydroxyl radicals (5) [13,39,59]:

$$h^+ + H_2O \rightarrow H^+ + {}^{\bullet}OH \quad (5)$$

Methanol is known to adsorb on $TiO_2$ [29] and other metal oxide catalysts [60] forming methoxy species (6). The latter may capture photogenerated holes to form methoxy radicals (7), which can further react with holes to release protons and form formaldehyde on the photocatalyst surface (8):

$$CH_3OH \rightarrow CH_3O_{(a)}{}^- + H^+ \quad (6)$$

$$CH_3O_{(a)}{}^- + h^+ \rightarrow CH_3O_{(a)}{}^{\bullet} \quad (7)$$

$$CH_3O_{(a)}{}^{\bullet} + h^+ \rightarrow CH_2O_{(a)} + H^+ \quad (8)$$

Results of the present study indicate that the so formed formaldehyde species do not desorb in the liquid phase but remain on the photocatalyst surface where they are subject to further oxidation. It has been proposed that formaldehyde adsorbs on $TiO_2$ through lone pair donation from the oxygen of carbonyl to Lewis acid sites of $TiO_2$ ($Ti^{4+}$ surface cations) [53]. As a result, the carbon atom of the carbonyl becomes more electrophilic, favoring the attack from a nucleophilic surface oxygen ion to form dioxymethylene (DOM) species (9), which has been detected in the DRIFTS spectra of Fig. 9:

$$CH_2O_{(a)} + O_{(s)} \rightarrow H_2CO_{2(a)} \quad (9)$$

It should be noted that surface oxygen ($O_{(s)}$) species required for the formation of DOM can be regenerated by the water splitting reaction. This is a reasonable suggestion because the photo-reforming reaction takes place under unaerated conditions, *i.e.*, in the absence of oxygen, and, therefore, $H_2O$ serves as the oxidizing agent [24].

Dioxymethylene produced according to reaction (9) may further consume photogenerated holes to produce formate species and release protons [29]:

$$H_2CO_{2(a)} + h^+ \rightarrow HCOO_{(a)} + H^+ \quad (10)$$

Finally, surface formate may be decarboxylated *via* the photo-Kolbe reaction [37,39,61,62] to yield protons and $CO_2$:

$$HCOO_{(a)} + h^+ \rightarrow H^+ + CO_2 \quad (11)$$

Protons formed in the above mentioned reactions are reduced by photogenerated electrons to yield $H_2$ in the gas phase according to reaction (4). The net result of the photo-reforming reaction is conversion of methanol and reaction intermediates into $H_2$ and $CO_2$, according to the stoichiometry of reaction (1).

## 4. Conclusions

Methanol can be photo-reformed efficiently into $H_2$ and $CO_2$ over $Pt/TiO_2$ photocatalyst suspensions irradiated by near UV light. The reaction rate depends strongly on the initial methanol concentration in solution and increases by more than two orders of magnitude with increase of $C_{MeOH}$ from zero to 1.0 M. The dependence of the reaction rate on $C_{MeOH}$ can be described by saturation-type kinetics according to the Langmuir-Hinselwood model. The hydrogen production rate increases with increase of photocatalyst loading and tends to stabilize for $C_{cat} > 3\ g\ L^{-1}$, due to the increased opacity of the suspension. For low values of $C_{MeOH}$, increase of the incident light intensity up to $2.3\ mW\ cm^{-2}$ results in an increase of the reaction rate, which is not affected significantly upon further increase of $I_0$. However, for high values of $C_{MeOH}$, $r_{H_2}$ shows a first order dependence on incident light intensity. The reaction proceeds *via* progressive oxidation of adsorbed methoxy species into $CO_2$, with intermediate formation of adsorbed formaldehyde, dioxymethylene and formate species. Protons liberated in these reactions are reduced by photogenerated electrons to yield $H_2$ in the gas phase. The net result is conversion of methanol and reaction intermediates into $H_2$ and $CO_2$, according to the stoichiometry of the methanol photo-reforming reaction.

## Acknowledgements

This research has been co-financed by the European Union (European Social Fund–ESF) and Greek national funds through the Operational Program "Education and Lifelong Learning" of the National Strategic Reference Framework (NSRF) - Research Funding Program: Thales. Investing in knowledge society through the European Social Fund (PhotoFuelCell project, MIS 379320).

## References

[1] A. Fujishima, K. Honda, Nature 238 (1972) 37–38.
[2] K.E. Karakitsou, X.E. Verykios, Journal of Physical Chemistry 97 (1993) 1184–1189.
[3] J.R. Bolton, Solar Energy 57 (1996) 37–50.
[4] M. Graetzel, Nature 414 (2001) 338–344.
[5] T. Bak, J. Nowotny, M. Rekas, C.C. Sorrell, International Journal of Hydrogen Energy 27 (2002) 991–1022.
[6] A. Kudo, Y. Miseki, Chemical Society Reviews 38 (2009) 253–278.
[7] M. Woodhouse, B.A. Parkinson, Chemical Society Reviews 38 (2009) 197–210.
[8] T. Kawai, T. Sakata, Nature 286 (1980) 474–476.
[9] M. Kawai, T. Kawai, K. Tamaru, Chemistry Letters 8 (1981) 1185–1188.
[10] M. Kawai, T. Kawai, S. Naito, K. Tamaru, Chemical Physics Letters 110 (1984) 58–62.
[11] K. Hashimoto, T. Kawai, T. Sakata, Journal of Physical Chemistry 88 (1984) 4083–4088.
[12] T. Sakata, T. Kawai, K. Hashimoto, Journal of Physical Chemistry 88 (1984) 2344–2350.
[13] A. Patsoura, D.I. Kondarides, X.E. Verykios, Catalysis Today 124 (2007) 94–102.
[14] D.I. Kondarides, V.M. Daskalaki, A. Patsoura, X.E. Verykios, Catalysis Letters 122 (2008) 26–32.
[15] V.M. Daskalaki, D.I. Kondarides, Catalysis Today 144 (2009) 75–80.
[16] A. Patsoura, D.I. Kondarides, X.E. Verykios, Applied Catalysis B 64 (2006) 171–179.
[17] N. Strataki, V. Bekiari, D.I. Kondarides, P. Lianos, Applied Catalysis B 77 (2007) 184–189.
[18] D.I. Kondarides, A. Patsoura, X.E. Verykios, Journal of Advanced Oxidation Technologies 13 (2010) 116–123.
[19] M. Cargnello, A. Gasparotto, V. Gombac, T. Montini, D. Barreca, P. Fornasiero, European Journal of Inorganic Chemistry (2011) 4309–4323.
[20] H. Bahruji, M. Bowker, P.R. Davies, F. Pedrono, Applied Catalysis B 107 (2011) 205–209.
[21] G.L. Chiarello, L. Forni, E. Selli, Catalysis Today 144 (2009) 69–74.
[22] G.L. Chiarello, D. Ferri, E. Selli, Journal of Catalysis 280 (2011) 168–177.
[23] V.M. Daskalaki, P. Panagiotopoulou, D.I. Kondarides, Chemical Engineering Journal 170 (2011) 433–439.
[24] P. Panagiotopoulou, et al., Catalysis Today (2012), http://dx.doi.org/10.1016/j.cattod.2012.09.029.
[25] V.M. Daskalaki, M. Antoniadou, G. Li Puma, D.I. Kondarides, P. Lianos, Environmental Science and Technology 44 (2010) 7200–7205.
[26] M. Antoniadou, V.M. Daskalaki, N. Balis, D.I. Kondarides, Ch Kordulis, P. Lianos, Applied Catalysis B 107 (2011) 188–196.
[27] G. Wu, T. Chen, W. Su, G. Zhou, X. Zong, Z. Lei, C. Li, International Journal of Hydrogen Energy 33 (2008) 1243–1251.
[28] J. Chen, D.F. Ollis, W.H. Rulkens, H. Bruning, Water Research 33 (1999) 669–676.
[29] T. Chen, Z. Feng, G. Wu, J. Shi, G. Ma, P. Ying, C.J. Li, The Journal of Physical Chemistry C 111 (2007) 8005–8014.
[30] T.A. Kandiel, R. Dillert, L. Robben, D. Bahnemann, Catalysis Today 161 (2011) 196–201.
[31] M. Bowker, L. Millard, J. Greaves, D. James, J. Soares, Gold Bulletin 37 (2004) 170–173.
[32] A. Dickinson, D. James, N. Perkins, T. Cassidy, M. Bowker, Journal of Molecular Catalysis A 146 (1999) 211–221.
[33] N.L. Wu, M.S. Lee, International Journal of Hydrogen Energy 29 (2004) 1601–1605.

[34] P. Panagiotopoulou, D.I. Kondarides, Journal of Catalysis 225 (2004) 327–336.
[35] P. Panagiotopoulou, D.I. Kondarides, X.E. Verykios, Journal of Physical Chemistry C 115 (2011) 1220–1230.
[36] P. Panagiotopoulou, A. Christodoulakis, D.I. Kondarides, S. Boghosian, Journal of Catalysis 240 (2006) 114–125.
[37] X. Fu, J. Long, X. Wang, D.Y.C. Leung, Z. Ding, L. Wu, Z. Zhang, Z. Li, X. Fu, International Journal of Hydrogen Energy 33 (2008) 6484–6491.
[38] L.S. Al-Mazroai, M. Bowker, P. Davies, A. Dickinson, J. Greaves, D. James, L. Millard, Catalysis Today 122 (2007) 46–50.
[39] X.J. Zheng, L.F. Wei, Z.H. Zhang, Q.J. Jiang, Y.J. Wei, B. Xie, M.B. Wei, International Journal of Hydrogen Energy 34 (2009) 9033–9041.
[40] J.-M. Herrmann, Catalysis Today 53 (1999) 115–129.
[41] A.V. Emeline, A.V. Rudakova, V.K. Ryabchuk, N. Serpone, Journal of Physical Chemistry B 102 (1998) 10906–10916.
[42] A.V. Emeline, V.K. Ryabchuk, N. Serpone, Journal of Physical Chemistry B 103 (1999) 1316–1324.
[43] A.E. Cassano, O.M. Alfano, Catalysis Today 58 (2000) 167–197.
[44] S.P. Kamble, S.B. Sawant, V.G. Pangarkar, Chemical Engineering Research and Design 84 (A5) (2006) 355–362.
[45] N. Serpone, A. Salinaro, Pure and Applied Chemistry 71 (1999) 303–320.
[46] A. Salinaro, A.V. Emeline, J. Zhao, H. Hidaka, V.K. Ryabchuk, N. Serpone, Pure and Applied Chemistry 71 (1999) 321–335.
[47] K. Okamoto, Y. Yamamoto, H. Tanaka, A. Itaya, Bulletin of the Chemical Society of Japan 58 (1985) 2023–2028.
[48] M.R. Nimlos, W.A. Jacoby, D.M. Blake, T.A. Milne, Environmental Science and Technology 27 (1993) 732–740.
[49] D.F. Ollis, in: E. Pelizzetti, M. Shiavello (Eds.), Photochemical Conversion and Storage of Solar Energy, Kluwer Academic Publishers, Dordrecht, 1990, pp. 593–622.
[50] J.G. Highfield, M.H. Chen, P.T. Nguyen, Z. Chen, Energy & Environmental Science 2 (2009) 991–1002.
[51] B.G. Frederick, G. Apai, T.N. Rhodin, Surface Science 277 (1992) 337–350.
[52] S. Bertarione, D. Scarano, A. Zecchina, V. Johanek, J. Hoffmann, S. Schauermann, J. Libuda, G. Rupprechter, H.-J. Freund, Journal of Catalysis 223 (2004) 64–73.
[53] T. Kecskés, J. Raskó, J. Kiss, Applied Catalysis A 273 (2004) 55–62.
[54] J. Raskó, T. Kecskés, J. Kiss, Journal of Catalysis 224 (2004) 261–268.
[55] L.J. Burcham, I.E. Wachs, Catalysis Today 49 (1999) 467–484.
[56] C. Zhang, H. He, Catalysis Today 126 (2007) 345–350.
[57] C. Cao, K.L. Hohn, Applied Catalysis A 354 (2009) 26–32.
[58] C. Zhang, H. He, K. Tanaka, Applied Catalysis B 65 (2006) 37–43.
[59] D.I. Kondarides, in: G. Centi (Ed.), Encyclopedia of Life Support Systems (EOLSS), Developed under the Auspices of the UNESCO, Eolss Publishers, Oxford, UK, http://www.eolss.net
[60] S.S. Akarmazyan, et al., Applied Catalysis B: Environmental (2012), http://dx.doi.org/10.1016/j.apcatb.2012.11.043.
[61] Y. Nosaka, K. Koenuma, K. Ushida, A. Kira, Langmuir 12 (1996) 736–738.
[62] B. Kraeutler, A.J. Bard, Journal of the American Chemical Society 100 (7) (1978) 2239–2240.